

Dissolution of Uranium Alloys in Nitric Acid

E. A. Kolobov^a, M. Yu. Kirshin^a, and Yu. A. Pokhitonov^{a,*}

^a *Khlopin Radium Institute, St. Petersburg, 194021 Russia*

**e-mail: yapokhitonov@mail.ru*

Received June 24, 2020; revised December 29, 2020; accepted December 12, 2021

Abstract—The dissolution of uranium alloys with Mo, Zr, Si, and other alloying elements in nitric acid has been studied. Data on the dissolution rate vs. the concentration of nitric acid and temperature are reported. The temperature coefficients of the reaction and the values of the effective activation energy of the interaction of alloys with an acid are calculated. For most of the samples, the obtained values are comparable with the dissolution rate of undoped uranium. In the case of introducing alloying elements Zr and Nb into metallic uranium, a decrease in the rate of the process occurred, and the rate of dissolution of uranium silicide was 5–10 times higher than that of undoped uranium. Upon dissolution, insoluble precipitates formed, their yield reached 8–10%. A relationship was established between the composition of inclusions present in the alloy and the composition of the precipitate after dissolution.

Keywords: dissolution of uranium alloys, uranium silicide, composition of precipitates, uranium alloys with molybdenum, zirconium, silicon

DOI: 10.1134/S1066362221050040

INTRODUCTION

Uranium metal was used as a nuclear fuel at a very early stage in the development of the nuclear industry in plutonium production reactors, research reactors, and nuclear power plants. But very soon it became obvious that the use of uranium, which has three allotropic modifications, is limited due to the tendency to shape change (swelling) under the influence of radiation and temperature fluctuations. A high rate of gas swelling brings about an increase in pressure on the cladding, which significantly limits the permissible level of fuel burnup. Improving the properties of metallic uranium can be achieved by introducing elements that promote the formation of solid solutions or intermetallic compounds and strengthen the metal as a result of dispersion hardening. The elements that make up uranium alloys should have a minimum neutron capture cross section, which makes it possible to reduce the loading of enriched uranium into the reactor [1–3].

At the present time, the main fuel material for nuclear power plants is UO₂ pellet fuel and, it would seem, there is no reason to expect changes in the current situation in the coming decades. Nevertheless, in many countries,

options are developed for the use of fuel compositions with metallic fuel in the form of U–Mo, U–Zr, U–Zr–Nb, and U–Pu–Zr alloys for fast neutron reactors, WWER reactors, and research reactors of various types [4–7]. Small nuclear power plants (SNPP) [8], which are one of the strategic directions of development of the State Corporation “Rosatom” are a large promising area for the use of fuel compositions with metal fuel.

At the moment, the potential demand of the small-scale energy market in Russia is estimated at approximately 9–12 GW, and by 2030 this value may increase by another 21 GW. There is also a great interest in SNPP on the international market. The increased interest in the use of uranium alloys in such plants is associated with the possibility of significant increasing the uranium content in the fuel composition and with an effort to limit the use of highly enriched uranium.

Due to the small (compared to oxide) volume of metal fuel, its processing is not a primary task. At the same time, upon expanding the areas of use and enhancing the unloaded irradiated fuel volumes, the question of its reprocessing will arise. And the most radical solution to the problem will be its processing at a radiochemical plant using existing or updated technologies. And in

this case, it will be necessary to take into account the peculiarities of metal compositions. The initial presence of metals in the fuel will result in the formation of an increased amount of precipitation during dissolution and subsequent operations, for example, at evaporating HLW solutions.

In view of the aforesaid this work was aimed at determining the conditions for dissolution of uranium alloy samples as well as the weight and composition of the formed precipitates.

EXPERIMENTAL

Samples of fuel claddings and cores made of metallic uranium and its alloys were manufactured at the Kharkov Institute of Physics and Technology. Melting of alloys was carried out in beryllium oxide crucibles heated by a resistance furnace and placed in a vacuum chamber with a rarefaction parameter of 10^{-5} mmHg. The melt temperature was 1450–1550°C, the keeping time was from 0.5 to 2 h, depending on the alloy composition. Casting was carried out into water-cooled copper molds. Moldings (cylinders 10 mm in diameter and 115–120 mm in height) were turned, and rods 6.5 mm in diameter were extruded from them at 900–1000°C. The operation was performed under a vacuum of 0.1 mmHg. Samples alloyed with aluminum, as well as aluminum, chromium, niobium, and tin were hardened and annealed. The heat treatment of medium-alloyed samples with titanium, zirconium, niobium, and aluminum consisted in homogenizing annealing at a temperature of 500–900°C for 100 h, followed by quenching in water. Alloys of uranium with silicon were annealed in the gamma phase for 50 h at 800–820°C.

Experiments on the study of the kinetics of dissolution of samples were carried out in a glass apparatus with a jacket (for thermostating the solution), equipped with a reflux condenser. Before the experiment, the sample surface was cleaned and etched with 6–8 M HNO₃. In experiments to determine the initial dissolution rates, the amount of material that passed into the solution did not exceed 80–100 mg (the weighed sample 4–10 g). Under these conditions, the value of the sample surface area was considered constant during the experiment. The process was monitored by periodically weighing the samples and analyzing the solution for uranium content. The formed precipitates were filtered off, washed with acid and alcohol, dried and weighed. To find out the

loss of uranium by precipitation, the precipitates were dissolved in a mixture of nitric and hydrofluoric acids, then the uranium content in the solution was determined.

To detect the amount and composition of precipitates formed upon dissolution we used the same alloy samples as in experiments on the kinetics of dissolution. The pre-weighed sample was placed in a glass flask with a reflux condenser, into which the calculated amount of acid was poured. The weight of the samples in some experiments ranged from 5 to 10–30 g. Dissolution, as a rule, was carried out at the boiling point of the solution. The resulting solution was separated from the precipitate by filtration through a paper filter. The content of uranium and nitric acid was found in the solution. The filter cake was washed with nitric acid, which concentration was close to the acid concentration in the solution after dissolution, and with water. Then it was dried to constant weight in an oven at a temperature of $90 \pm 5^\circ\text{C}$ and weighed.

RESULTS AND DISCUSSION

Dissolution of uranium-molybdenum alloys. To date, the dissolution of uranium-molybdenum alloys has been studied most fully. The alloy of uranium with 9 wt % molybdenum (OM-9) has been well studied and successfully used for a long time in the fuel elements of the Obninsk and Bilibino NPPs and in the AMB reactor at the Beloyarsk NPP.

We used alloy samples cut off on a lathe from the control (witness) fuel element. Before dissolution, the cladding of the fuel element and the calcium layer were removed from the samples.

The data on the dissolution rate of the uranium-molybdenum alloy vs. the acid concentration are shown in Fig. 1.

The plot of the dissolution rate vs. acidity of the solution in logarithmic coordinates demonstrate that the slope of the straight line is 2.0 ± 0.1 . The initial dissolution rate of the alloy at first rather sharply rises with an increase in the concentration of nitric acid, and at a concentration of 10–12 M the growth slows down, and an increase in acidity has a lesser effect.

As already noted, the dissolution process is often complicated by the formation of insoluble compounds. In our case, the dissolution of the studied samples in concentrated nitric acid was accompanied by the formation of a white precipitate. When treating the alloy

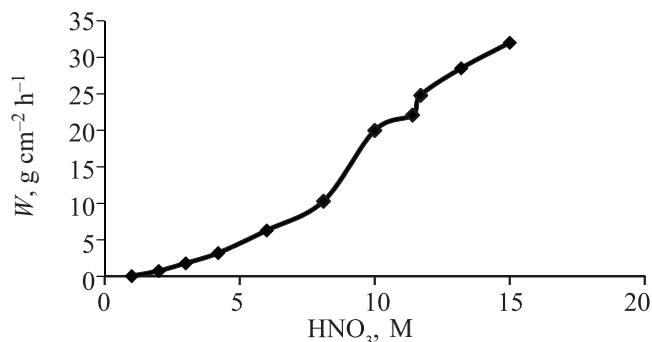


Fig. 1. The dissolution rate W of the uranium–molybdenum alloy at 90°C vs. the nitric acid concentration.

with nitric acid solutions, a bulk film of molybdenum oxide forms on the sample surface, which hinders the access of reagents to the material being dissolved.

The interaction rate of the uranium alloy with nitric acid, as expected, increases with the temperature of the experiment. The experimental points obtained when determining the initial dissolution rate of the samples in the temperature range 60–90°C fit well on a $\log W-1/T$ straight line. The slope of the straight line characterizes the apparent activation energy (E) of the process. The calculated value of E turned out to be 5900 ± 500 cal/mol, the temperature coefficient was 1.3.

Note that during the alloy dissolution the accumulation of uranium and molybdenum salts in the solution occurs, which also affect the course of the process. Initially, with increasing the content of uranyl nitrate in the solution, the reaction rate increases, apparently due to the catalytic action of the uranyl ion on the process. The maximum value of the dissolution rate is in the uranium concentration range of 0.6–0.8 M. A further increase in the concentration of uranium in the solution leads to a decrease in the solubility of molybdenum and, probably, to the formation of a film of poorly soluble molybdic acid on the sample surface, which hinders the access of the reagent to the sample.

The effect of the concentration of nitrate ions on the dissolution was studied. The dissolution rate of the uranium-molybdenum alloy in nitric acid was $2.1-2.2$ g cm⁻² h⁻¹ ($[\text{HNO}_3] = 4.2$ M) and did not depend on the NaNO_3 concentration in the range from 0.25 to 1 M.

A decrease in the concentration of free nitric acid and the accumulation of reaction products during the dissolution result in the formation of a solid phase in the uranium–molybdenum solution. The chemical analysis of

the precipitates showed that the content of uranium and molybdenum in them is 41.0 and 31.7%, respectively, which corresponds to the formula $(\text{UO}_2)_2\text{Mo}_6\text{O}_{21}$.

Data on the effect of the HNO_3 concentration and temperature on the $\text{MoO}_3 \cdot \text{H}_2\text{O}$ solubility are reported in [9–11]. The maximum $\text{MoO}_3 \cdot \text{H}_2\text{O}$ solubility is at the HNO_3 concentration of 4–6 M, and with increasing the temperature from 20 to 100°C the solubility diminishes. It was also shown that in ~ 1.5 M HNO_3 at 25°C the $\text{MoO}_3 \cdot \text{H}_2\text{O}$ solubility in the range from 0 to 0.95 M of uranium is practically independent of its concentration. With increasing the HNO_3 concentration to 3 M the $\text{MoO}_3 \cdot \text{H}_2\text{O}$ solubility increases, and at the HNO_3 concentration of 3–5 M the solubility reaches a plateau or passes through a maximum, depending on the concentration of uranium.

It should be noted that in the case of dissolution of irradiated fuel, it is the presence of molybdenum and zirconium that is the most important factor in the formation of the precipitates at all stages of spent nuclear fuel (SNF) reprocessing. The formation of zirconium molybdate precipitates depends on many factors (for example, on the composition of the solution, acid concentration, etc.) [12–14].

The behavior of Mo and Zr in highly concentrated solutions of uranyl nitrate, depending on the solution composition, temperature, and time of its keeping, is report in [15]. Analysis of the available data indicates that the precipitation is a multistage polymerization process, and the change in the forms of Mo in solution occurs at any temperature, but at various rates. The lack of precipitate formation can be caused just by the delay in its formation, but the process can resume, which leads to secondary precipitation [14, 15]. When the solutions stand, the processes of further precipitation take place. Data on the formation of secondary precipitates and their composition upon dissolution of irradiated oxide fuel are reported in [16].

Dissolution of samples of uranium alloys with zirconium and some other alloying elements. As already noted, the metallic fuel in the form of U–Zr, U–Zr–Nb, and U–Pu–Zr alloys is considered as promising fuel material for LWR reactors, fast reactors, and small nuclear power plants. Therefore, in addition to the uranium–molybdenum alloys we studied the dissolution of alloys with Zr and some other alloying elements in nitric acid. For a comparative analysis of the effect

Table 1. Effect of temperature on the initial dissolution rate W of uranium and its alloys with zirconium in 6 M HNO₃

Content of the alloying elements in uranium, wt %	Temperature, °C	W , g m ⁻² h ⁻¹	Activation energy, kJ mol ⁻¹	Temperature coefficient K
Undoped uranium	20	8.3 ± 0.7	63 ± 12	2.0
	70	610 ± 60		
	80	1220 ± 80		
	90	1790 ± 60		
Zr 1.0	20	9.6 ± 0.9	56 ± 10	1.9
	70	430 ± 70		
	80	840 ± 120		
	90	1130 ± 90		
Zr 2.6	70	120 ± 40	76 ± 20	2.0
	80	250 ± 80		
	90	520 ± 80		
Zr 2.5, Nb 1.55	70	72 ± 23	142 ± 19	4.4
	80	320 ± 160		
	90	1120 ± 310		
Zr 1.9, Nb 2.03, Al 1.0	70	42 ± 4	124 ± 60	2.7
	60	110 ± 12		
	70	460 ± 50		
Zr 2.0, Nb 2.0, Al 0.5	50	250 ± 20	120 ± 30	4.5
	70	1140 ± 210		
	80	1390 ± 30		
Zr 5.0, Al 0.5	20	1.7 ± 0.7	80 ± 20	2.8
	70	310 ± 20		
	80	770 ± 70		
Zr 5.0, Nb 1.5, Sn 0.5	20	28.4 ± 5.5	63 ± 20	2.3
	70	390 ± 20		
	80	1120 ± 40		
	90	2000 ± 240		

of alloying elements on the dissolution rate of alloys, the temperature dependences of the dissolution rate in 6 M HNO₃ were constructed. The experimental data are listed in Table 1.

As can be seen from the data obtained, the introduction of alloying elements into uranium leads to a significant reducing the initial dissolution rate. At the same time, no clear correlation between the content of alloying elements and the dissolution rate of alloys was revealed.

The temperature coefficient and activation energy were calculated from the temperature dependence of the dissolution rate ($K = 1.9$ – 4.5 and $E = 60$ – 140 kJ mol⁻¹). No unambiguous relationship between K and E with the alloy composition was also revealed.

In addition to the U–Mo(Zr) alloys discussed above, a series of experiments were carried out to study the

dependences of the dissolution rate and precipitation for compositions with Si. For the uranium silicide samples with different Si contents the initial dissolution rates in nitric acid (4–12 M) and in the temperature range of 40–90°C were found (Table 2). A distinctive feature of alloys with Si is an increase in the dissolution rate in comparison with metallic uranium. In various series of experiments, the difference was 4–8 times. The samples did not differ so much between themselves: in 6 M HNO₃ the rates differed by about a factor of 2. However, like the dissolution of alloys with Zr, no clear correlation was found between the Si content and the change in the dissolution rate.

The values of the calculated activation energy E are in the range of 30–80 kJ mol⁻¹, the temperature coefficient K is 2.0–1.4.

Table 2. Effect of acid concentration and temperature on the initial dissolution rate W of uranium–silicon alloys

Content of the alloying elements in uranium, wt %	Dissolution conditions		W , g m ⁻² h ⁻¹	Activation energy, kJ mol ⁻¹
	acid concentration, M	temperature, °C		
Undoped uranium	6.0	20	8.3 ± 0.7	63 ± 12
	6.0	70	610 ± 60	
	6.0	80	1220 ± 80	
	6.0	90	1790 ± 60	
	7.9	70	1330 ± 70	
	12.2	70	4450 ± 70	
Si 2.7	4.0	50	1340 ± 100	54 ± 8
	4.0	70	3200 ± 300	
	6.0	50	1700 ± 900	
	6.0	70	6500 ± 200	
	8.0	50	6300 ± 1400	
	10.0	70	22800 ± 8400	
Si 3.2	4.0	70	3000 ± 600	43 ± 5
	6.0	40	960 ± 240	
	6.0	50	2100 ± 400	
	6.0	80	8500 ± 800	
	6.0	90	11300 ± 200	
	8.0	50	9600 ± 2500	
	8.0	70	10100 ± 3000	
	10.0	70	12600 ± 1200	
Si 3.8	12.1	70	19200 ± 3000	33 ± 5
	6.0	50	2700 ± 600	
	6.0	70	5100 ± 700	
	6.0	80	8200 ± 700	
	8.0	70	7100 ± 700	
	12.2	70	13200 ± 2400	
Si 3.7, Al 1.2	4.0	70	460 ± 70	40 ± 12
	6.0	60	2800 ± 1800	
	6.0	70	4500 ± 2100	
	6.0	80	5600 ± 3200	
	8.0	70	7800 ± 340	
	10.0	70	11040 ± 660	
Si 3.8, Al 1.2, Al 0.1, Nb 0.18	6.0	50	320 ± 70	84 ± 50
	6.0	70	3000 ± 1800	
	6.0	80	5400 ± 3000	
	8.0	70	6000 ± 2400	
	10.0	70	10800 ± 2400	

Table 3. Dissolution rate of uranium alloy samples in nitric acid with addition of hydrofluoric acid (temperature 70°C)

Content of the alloying elements in uranium, wt %	The initial dissolution rate of the samples, $\text{mg cm}^{-2} \text{ min}^{-1}$, at acid concentration, M		
	6.0 HNO_3	6.0 $\text{HNO}_3 + 0.05 \text{ HF}$	6.0 $\text{HNO}_3 + 0.1 \text{ HF}$
Al 0.1, Cr 0.15	0.3	5.5	11.5
Al 0.1, Cr 0.015, Sn 0.5, Ge 0.35	4.8	6.0	7.5
Al 0.07, Mo 0.1, Nb 0.08, Sn 0.07, Zr 0.05	0.2	3.6	10.4
Si 3.8	9.2	8.0	6.5
Si 3.7, Al 1.1	9.8	6.7	5.1
Zr 2.6	0.7	2.8	5.1
Zr 1.9, Nb 2.3, Al 1.0	0.4	1.4	2.7
Ti 5.0	0.2	4.9	7.0

For all samples the dissolution reaction in nitric acid, at least in the initial period, proceeds in the kinetic region. Upon the dissolution the role of diffusion processes increases due to the formation of the film on the surface.

In contrast to undoped uranium the dissolution was accompanied by the formation of loose peelable precipitates on the surface. In some cases, the sample retained its original shape until the end of dissolution.

In conclusion of this section, it should be noted that the temperature dependence of the dissolution rate of uranium alloys is most pronounced for samples (1) with beryllium oxide and (2) with small additives of Mo, Sn, Zr, Nb: the temperature coefficient of these samples was 3.1 and 5.0, respectively.

A wide variety of the investigated compositions and the lack of samples containing only one additive, but in different quantities, does not allow definite conclusions about the effect of one or another element on the rate of the process.

Another difficulty in explaining the results obtained is the double influence of the presence of even one element. On the one hand, impurity atoms affect the energy of the crystal lattice of uranium itself, which probably results in the increase in the dissolution rate. At the same time, the alloying elements can affect the composition of the surface oxide layer and thereby lead to passivation of the sample surface.

Note that in some cases alloying elements are capable of forming chemical compounds with uranium, which the dissolution rate can differ greatly. The fact that a homogeneous alloy has the same properties in all directions refers to macroproperties. A chemical or

electrochemical reaction is the result of the interaction of atoms, ions or molecules at the micro level.

Almost always, the partial electrochemical properties of the alloy constituents differ, thus, there is always a thermodynamic probability of selective dissolution of the alloy constituents. This conclusion can also be applied when considering the real systems. The dissolution pattern is complicated in many respects due to the formation of insoluble compounds already at the beginning of the reaction with the acid. The issues of uneven distribution of impurities in the alloy itself (alloying elements in uranium) will be considered below when discussing the composition of the formed precipitates.

In the conclusion of this section, we present the experimental data on the dissolution of alloys in nitric acid with the addition of hydrofluoric acid. As known the hydrofluoric acid (or salt) additives are used for dissolving zirconium-containing materials: For example, the method of dissolution in a mixture of fluoride and ammonium nitrate (Zirflex process) is considered promising in the case of selective removal of zirconium claddings. To dissolve samples of alloys with Zr, Nb, and Si, we used solutions of nitric acid with the addition of hydrofluoric acid in amounts of 0.05–0.1 M.

Data on the dissolution rate of alloys at 70°C are listed in Table 3. The addition of hydrofluoric acid led to an increase in the dissolution rate of zirconium–niobium alloys by a factor of 10–50. Some samples dissolved without the precipitate formation, but it was not possible to achieve complete dissolution of all studied samples.

The action of hydrofluoric acid is associated with the destruction of the surface acid-resistant oxide layer,

Table 4. Yield and composition of precipitates after dissolution of alloys with zirconium and other alloying elements in 9 M HNO₃

Sample parameter	Dissolution conditions		Precipitate after the dissolution		
	weighed sample, g	time of complete dissolution,	% by weight of the sample	loss of uranium with precipitate, %	precipitate composition, %
Al 0.1, Cr 0.15	10.7	~30	0.24	0.015	
Al 0.1, Cr 0.015, Sn 0.5, Ge 0.35	9.57 65.8	2–3	0.16	0.005	Al 0.25, Si 16.6, SnO ₂ 2.8, Cr 2.6, Mo 4.7
Al 0.07, Mo 0.1, Nb 0.08, Sn 0.07, Zr 0.05	16.1 57.6	13	0.24 0.4	0.02 0.003	Nb 18, Al 1.4, Cr 8.4, Nb 36, Zr 1.0, Sn 2.2, Mo 0.05
Zr 2.6	13.2 4.2	~15 6–8	0.21 4.3		Zr 30
Zr 2.5, Nb 1.55	9.34	~26	8.2		
Zr 1.9, Nb 2.3, Al 1.0	3.2	9–10	5.9	0.17	
Ti 5.0	4.05 ^a	59.7% for 24 h	3.9	0.02	
Zr 2.0, Nb 2.0, Al 0.5	3.48 ^a	88% for 4 h	3.7		
Zr 1.0	32.4		0.7		Zr 30.0, Cr 4.5, Si 3.2
Zr 5.0, Al 0.5	6.16 19.8	8–9 25–30	2.6 2.2		
Zr 5.0, Nb 1.5, Al 0.5, Sn 0.5	7.8		5.0		

^a Dissolution was conducted in 6 M HNO₃.

dissolution of which is accompanied by the formation of Zr, Nb, and partly U fluoride complexes.

The formation of insoluble residues occurs in almost all cases of dissolution of uranium alloys.

The amount and composition of insoluble precipitates during the dissolution of alloys. Along with the dissolution rate, the amount of precipitates and their composition (including the content of fissile materials in them) are important parameters in the opening the irradiated fuel and its preparation for subsequent reprocessing. The purpose of the following experiments was to determine the amount and composition of precipitates obtained after dissolving uranium alloys in nitric acid solutions.

As expected, the yield of precipitates upon dissolution of alloys is determined by the amount and composition of alloying elements. If, upon dissolution of oxide fuel compositions (or metallic uranium), the formation of precipitates is determined by burnup (an increase in the concentration of fission products), then in the dissolution of alloys, an opportunity for precipitation takes place in unirradiated samples since precipitating elements are present initially in the fuel. The results of the

analysis of precipitates after dissolution of the alloys are presented in Table 4.

In a number of experiments along with the weight of insoluble precipitates, their composition has also been analyzed: The basis is made up of multivalent metals, which can react with oxygen and form poorly soluble compounds.

The yield the precipitates depending on the core composition and the conditions of dissolution, varies within 0.02–8.2% of the weight of the dissolved samples. All precipitates contain a large amount of zirconium. In the case of niobium and tin additions to the alloy these elements were also found in the composition of the precipitates. The total losses of uranium did not exceed 0.2%.

The analysis on the solutions after the dissolution of the uranium–silicon compositions (Table 5) indicate that only an insignificant amount of silicon passes into the solution, and the main part (more than 99.9%) remains in the precipitate, in the form of oxide.

In general, the transition of Si into solution is determined by the proceeding of two coupled reactions. First, the oxidation of Si present in the alloy occurs

with the formation of $\text{SiO}_2 \cdot n\text{H}_2\text{O}$ -type compounds, then a chemical dissolution reaction follows, including the stage of Si–O–Si bond cleavage with the formation of silicic acid. According to the analysis of uranyl nitrate solutions (80–250 g/L) obtained after dissolving alloys with Si in nitric acid, the Si content in them was from 10 to 120 mg/L.

In the course of the work, the question arose about the relationship between the formation of precipitates upon dissolution with the structural features of the initial material.

An inhomogeneous distribution of inclusions of alloying elements in uranium alloys was reported in [17]. The authors studied the distributions of alloying elements (Zr and Nb) and carbon in the material of the uranium fuel core. Uranium of a corrected composition and two of its alloys (U + 2.5 wt % Zr + 1.6 wt % Nb and U + 2.7 wt % Nb, which is quite similar in composition to one of the samples taken in our work) were used as the investigated materials for casting.

In the process of obtaining ingots, no uniform distribution of carbon and alloying impurities occurs. A characteristic feature of these materials consisted in the fact that carbon in them was in the form of various compounds. The authors believe that in undoped uranium carbon was in the form of uranium carbide, and in the alloy with Zr and Nb alloying elements, in the form of zirconium and niobium carbides, respectively, which is due to the different affinity of elements for carbon [17].

Metallographic studies of the uranium structure of a corrected composition in the initial state showed

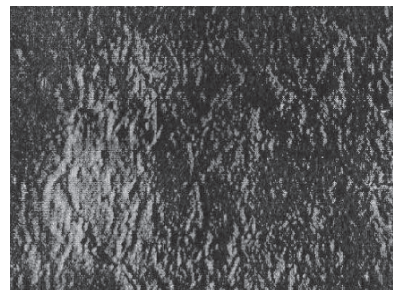


Fig. 2. Microstructure of uranium alloy with 4.9 wt % Zr and 1.5 wt % Nb (magnification $\times 1000$, secondary electrons).

that most of the inclusions in the matrix were uranium carbides. On samples after their treatment by centrifugal casting, there was an increased content of uranium carbides in the region of the central hole. Their particles were close in shape and size to similar particles in the initial material. The Zr concentration in the region of the central hole after keeping during centrifugal casting was 0.4, 5.3, 8.8, and 10.8 wt %. Thus, the authors conclude that in the process of centrifugal casting of metallic uranium, along with the alloying uranium with zirconium, the decomposition of uranium carbides and the formation of zirconium carbides occur. Almost all carbon as a result of centrifugal casting of alloys accumulates in the region of the central hole in the U + 2.5 wt % Zr + 1.6 wt % Nb alloy in the form of zirconium carbide and in the U + 2.7 wt % Nb alloy in the form of niobium carbide [17].

Figure 2 shows the results of metallographic study of the structure of the uranium alloy U + 4.9 wt % Zr + 1.5 wt % Nb + 0.2 wt % C + 0.03 wt % Fe + 0.01 wt % Ni + 0.01 wt % Al + 0.06 wt % Si + 0.5 wt % Sn.

Table 5. Yield and composition of precipitates after dissolution of alloys with silicon in 9 M HNO_3

Sample parameter	Weight of the sample, g	Precipitate after the dissolution		
		% by weight of the sample	loss of uranium with precipitate, %	precipitate composition, %
Si 3.7	13.9	9.7	0.07	Si 29.0
	28.2	9.7	0.08	
Si 3.7, Al 1.2	22.0	9.4	0.02	Si 39.0
	41.0	11.8	0.76	
Si 3.8, Al 1.2, Nb 0.8	25.0	9.9	0.02	Si 2.5, Nb 1.3
	39.8	6.6	0.13	
Si 3.2	20.7	6.7		Si 34, Zr 1.4
Si 4.0	20.05	8.6		Si 25.0
Si 3.8	23.0	9.7	0.08	

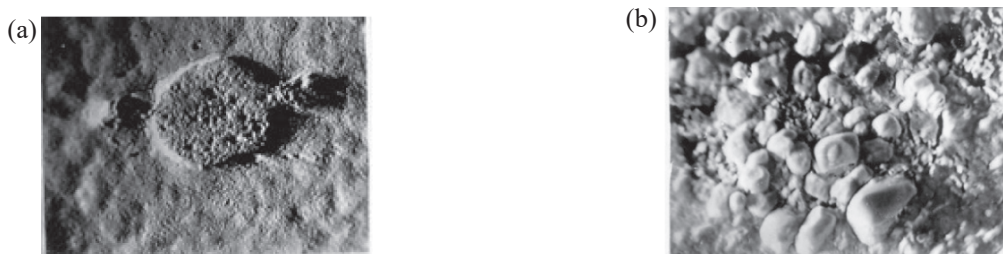


Fig. 3. (a) Microstructure of the U–Zr alloy with the inclusion area (magnification $\times 200$, secondary electrons); (b) inclusion microstructure (magnification $\times 1000$, absorbed electrons). The dark areas are the phase of the basic composition, the light areas are the phase enriched with zirconium, tin, and other elements.



Fig. 4. (a) Microstructure of the U–Zr alloy with the inclusion area (magnification $\times 200$, secondary electrons); (b) inclusion microstructure (magnification $\times 1000$, absorbed electrons). The dark areas are the phase of the basic composition, the light areas are the phase enriched with zirconium, tin and other elements.

Table 6. Results of the analysis of the macrocomposition of the initial sample, the composition of defect inclusions in the alloy, and the composition of the precipitates after dissolution

Sample no.	Content of uranium and alloying elements in the alloy			Notes
	uranus	zirconium	niobium	
1	95.46	2.91	1.63	Alloy composition according to the passport: Zr 4.9, Nb 1.5, C 0.20, Fe 0.03, Ni 0.01, Al 0.05; Si, 0.06, Sn 0.5 (uranium—the rest). The content of other elements was at the determination limit (oxygen, tin, silicon, iron, copper).
2	95.42	3.06	1.52	
3	96.07	2.67	1.27	
4	95.49	2.94	1.58	
5	95.60	2.81	1.49	
Average	95.60	2.88	1.50	
Analysis results of detected inclusions				
1	2.66	49.51		Sn 36.17, O 11.66
2		83.40	0.60	O 16.0
3		88.02	0.62	O 11.36
4	5.15	40.80	3.69	Sn 27.95, O 19, Cu 1.05
5	5.27	73.28	3.02	Sn 0.42, O 11.47, Si 0.29, Fe 0.36, Cu 0.34
6	14.58	40.75	0.55	Sn 28.55, O 14.2, Si 1.05
7	2.62	48.58		Sn 36.06, O 12.74
Composition of the precipitate after dissolution of the alloy				
1	10.96	70.95		O 15.68, Si 0.35
2	2.47	68.85		O 15.3, Si 1.38
3	36.26	49.80		O 13.8
4	10.44	71.24		O 13.8
5	31.36	58.20		O 6.9

Areas with inclusions were found during the study of the alloy structure and an analysis of their composition was carried out. Photographs of defects (inclusions) on the surface of a thin section of the alloy are shown in Figs. 3, 4.

Thus, it was demonstrated that there are macroinhomogeneities in the samples of uranium alloys.

In the composition of the inclusions, an excess of elements introduced during the production of the core was found, as well as oxygen and small amounts of silicon. The distribution pattern of chemical elements in the area with inclusions is presented in Table 6.

The studied sample was subjected to dissolution. The analysis of resulting precipitate (the yield about 5 wt %) showed that the losses of uranium with the precipitate were at the level of 0.8–1% of its content in the initial sample. The main elements that make up the precipitate were Zr, U, O, and Al. The result obtained allows assumption that the insoluble precipitate is not a mixture of hydrated oxides, but a complex chemical compound, composition of which is determined by the composition of inclusions initially present in the alloy, which was confirmed in the study of the initial sample.

Thus, the data obtained (Table 6) indicate a correlation between the chemical composition of inclusions and the composition of precipitates formed upon dissolution of the alloy core in nitric acid.

CONCLUSIONS

The reaction temperature coefficients and the effective activation energy of the interaction of uranium alloys with nitric acid were calculated based in the dependences of the initial dissolution rates on temperature. The results obtained did not make it possible to establish a clear correlation between the content of alloying elements in the alloys and the change in their dissolution rate.

For most of the samples, the obtained values are comparable with the dissolution rate of undoped uranium. When Zr and Nb alloying elements are introduced into metallic uranium, the rate of the process decreases. The dissolution rate of uranium silicide in 6 M nitric acid is approximately 5–10 times higher than that of undoped uranium.

When almost all of the studied samples are dissolved, insoluble precipitates with the yield 8–10% are formed, which leads to difficulties in the clarification of technological solutions before extraction and an increase

in uranium losses. Losses of uranium can be determined not only by adsorption on the sludge, but also by the possible formation of complex chemical compounds in the fuel and their precipitation during dissolution.

It was found that the reason for the formation of insoluble precipitates is the insufficient homogeneity of the initial alloy and the presence of inclusions enriched with alloying elements.

These difficulties do not impede the implementation of technological processes for reprocessing fuel based on uranium metal alloys. For a detailed study of the effect of the heterogeneity of the alloying element distribution on the composition of precipitates, it is necessary to carry out a set of studies considering the relationship between the phase composition of the fuel, its dissolution rate, and precipitation.

Similar studies should also be performed on irradiated alloy samples, which makes it possible to choose the regulations for the reprocessing of irradiated fuel and industrial waste.

SUPPLEMENTARY INFORMATION

The online version contains supplementary material available at <https://doi.org/10.1134/S1066362221050040>: Tables of the initial dissolution rates (W , g cm⁻² h⁻¹) of uranium–molybdenum alloy in nitric acid, data on the effect of sodium nitrate on the dissolution rate of uranium–molybdenum alloy; and also a figure illustrating the effect of temperature on the initial dissolution rate of uranium and its alloys.

CONFLICT OF INTERESTS

The authors declare that they have no conflicts of interest.

REFERENCES

1. Sokurskii, Yu.N., Sterlin, Ya.M., and Fedorchenko, V.A., *Uran i ego splavy* (Uranium and Its Alloys), Moscow: Atomizdat, 1976.
2. Reshetnikov, F.G., *Razrabotka tekhnologii polucheniya metallicheskogo urana i splavov na ego osnove, VNIINM – 50 let*, Moscow, 1995, vol. 1, pp. 113–123.
3. Solonin, M.I., Vatulin, A.V., and Stetskii, Yu.A., Abstracts of Papers, *XII ezhegodnoi konf. Yadernogo obshchestva Rossii “Issledovatel’skie reaktory: nauka i vysokie tekhnologii” 25–29 iyunya 2001 g.* (12th Annual Conf. of Nuclear Society of Russia on Research Reactors: Science and High Technologies, June 25–29, 2001), 2001.

4. Zhirnov, A.D., Sirotkin, A.P., Bryunin, S.V., Pushkarev, S.V., and Runin, V.I., *Atom. Energiya*, 1973, vol. 34, no. 6, pp. 479–481.
5. Sirotkin, A.P., *Atom. Tekhnika za Rubezhom*, 1984, no. 3, pp. 3–13.
6. Kim, Sang-Ji, Kim, Young-Jin, Kim, Young-H, and Park, Chang-Kue, *J. Nucl. Sci. Technol.*, 1999, vol. 36, no. 5, pp. 459–469.
7. Krasnorutskii, V.S. and Tatarinov, V.R., *Vopr. Atom. Nauki i Tekhniki. Ser.: Fizika Radiatsionnykh Povrezhdenii i Radiatsionnoe Materialovedenie*, 1999, nos. 1–2(73–74), pp. 87–94.
8. *Vozvrashchenie reaktorov maloi moshchnosti* (Return of Low Power Reactors), *Atom. tekhnika za rubezhom*. 2003, no. 3, pp. 25–28.
9. Ferris, L.M., *J. Chem. Eng. Data*, 1961, vol. 6, pp. 600–603.
10. Meerson, G.A. and Mikhailova, V.G., *Zh. Neorg. Khim.*, 1967, vol. 12, pp. 1615–1618.
11. Doucet, F.J., Goddard, D.T., Taylor, C.M., et al., *Phys. Chem. Chem. Phys.*, 2002, vol. 4, pp. 3491–3499.
12. Akhmatov, A.A., Zil'berman, B.Ya., Fedorov, Yu.S., et al., *Radiochemistry*, 2003, vol. 45, no. 6, pp. 523–531. <https://doi.org/10.1023/B:RACH.0000015756.24385.6d>
13. Magnaldo, A., Masson, M., and Champion, R., *Chem. Eng. Sci.*, 2007, vol. 62, pp. 766–774.
14. Maslennikov, A.G., *Doctoral Sci. (Chem.) Dissertation*, Moscow, 2008.
15. Khonina, I.V., Lumpov, A.A., Shadrin, A.Yu., Zil'berman, B.Ya., and Kravchenko, N.G., *Radiochemistry*, 2010, vol. 52, no. 2, pp. 151–154. <https://doi.org/10.1134/S1066362210020104>
16. Burakov B.E, Pokhitonov Yu.A, Ryazantsev, V.I., Savin, R.A., Saprykina, V.F., and Rens, P.D., *Radiochemistry*, 2010, vol. 53, no. 4, pp. 342–345.
17. Belash, N.N., Tatarinov, V.R., Ragulina, N.I., Semenov, N.A., and Danilova, O.V., *Vopr. Atom. Nauki i Tekhniki. Ser.: Fizika Radiatsionnykh Povrezhdenii i Radiatsionnoe Materialovedenie*, 2002, no. 3(81), pp. 88–93.